Fabrication and electrical properties of FTO Nano-particles/Nano-crystal porous silicon heterojunction under gamma radiation effect

Hasan A.Hadi

Department of Physics, College of Education, Al-Mustanseriyah University, (IRAQ)
E-mail: ha_yab@yahoo.com

ABSTRACT

In this paper porous silicon layer was papered by photo electrochemical etching PECE with laser assisted and the FTO thin film deposited on porous silicon layer substrates by spray pyrolysis technique. To study the effect of gamma radiation on electrical and photocurrent characteristics' of fluoride tin oxides /porous silicon /mono crystalline silicon n-type heterojunction was exposed to 60 Co-ray sources at room temperature. The FTO/PS/n-Si/Al heterojunction was study using $I - V$ and $C^{-2} - V$ measurements, with focus on the influence of the duration gamma radiation on the electrical properties. © 2015 Trade Science Inc. - INDIA

KEYWORDS

Porous silicon;
Photo-electrochemical etching;
Spray pyrolysis;
Thin film;
Heterojunction.

INTRODUCTION

Electrochemical etching is one of the simplest and most reliable methods used to synthesis porous silicon PS[1]. Typically, the PS layer is sandwiched between the c-Si substrate and a metallic contact.the PS layer was considered to behave like a wide band gap semiconductor and assumed a Schottky barrier formed between the metal and the PS. In some cases, these metal contacts are replaced by transparent conductive oxide (TCO), such as tin oxide[2] or zinc oxide[3] today, the nonporous silicon is very interesting material for both its optical and electrical properties[4]. PS and FTO, exhibit an elevated specific surface; they are potentially attractive for these types of applications. It is expected that combining both materials in a single device will lead to an enhancement of their sensing properties[5]. Among the various deposition techniques, spray pyrolysis is well

suited for the preparation of doped tin oxide thin films because of its simple and inexpensive experimental arrangement, ease of adding various doping materials, reproducibility, high growth rate and mass production capability for uniform large area coatings[6]. Fluoride ten oxide has numerous applications because of their high optical transparency in the visible region, good electrical conductivity and the high infrared reflectivity[6-9]. Irradiation with gamma rays changes the physical properties of the materials which they penetrate. The changes are strongly dependent on the internal structure of the absorbed substances. It is believed that ionizing radiation causes structural defects leading to their density change on the exposure to γ-rays[10]. In this work, FTO (SnO_2 :F) thin film was prepared by the chemical spray pyrolysis technique, at a normal atmospheric pressure on a glass substrate and porous silicon PS layer substrate. PS was prepared by photo-electrochemical

etching (PECE) technique. The structural and morphology of porous layer and FTO thin film were measured by XRD, SEM, AFM, and optical microscopy. Electrical properties of the FTO/PS/n-Si heterojunction were studied before and after gamma-ray irradiation, with different exposure periods (7, 14, and 21) days.
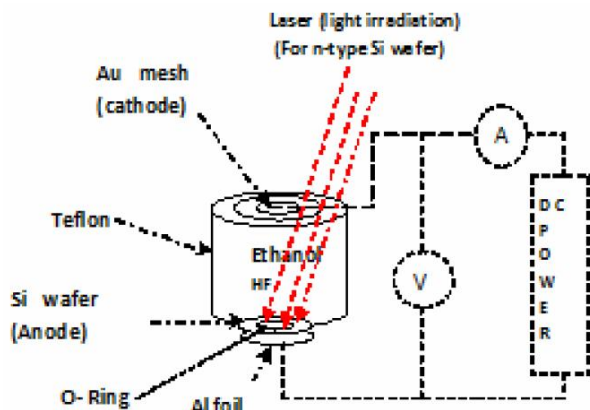

Figure 1 : Schematic of the single cell back-side setup to fabrication of porous silicon

EXPERIMENTAL

Prepared porous silicon PS

The single cell back-side contact and has been already shown in Figure 1 was used to papered porous layer. In this cell, the Si wafer is placed on a copper disk and sealed through an O-ring, so that only the front side of the sample is exposed to the electrolyte. The copper disk has to be cleaned with a lapping machine in order to remove the oxide film that forms itself after many etching processes. This geometry is particularly indicated for a uniform illumination of the sample during the etching. The PS layer was fabricated by anodic etching of a silicon wafer n-type substrate, orientation (100) and a resistivity of 17Ω cm corresponding $2.59 \times 10^{14} \ cm^{-3}$ .etching cell using a mixture of aqueous hydrogen fluoride (purity 40%) and methanol (purity 99%), 1:1 by volume. The silicon was used as an anode while the cathode was of gold mesh to papered porous layer by photo electrochemical etching (PECE) technique. The silicon surface was etched with a current density of $\frac{7 \, mA}{cm^2}$ for 3 min under exposure to incandescent red laser light (650nm-30mW) during the etching.

Prepared fluoride tin oxide FTO

The chemical spray pyrolysis experimental setup is similar to the standard one which is shown in Figure2, is a versatile as well as a low-cost technique that has been used to deposit semiconductor films. In this process, a thin film is deposited by spraying a solution on a hot surface. The constituents react to form a chemical compound. Thin layers (113nm) of fluorine doped tin oxide (FTO) have been prepared on Microscopic glass slides ($2.5 \times 2.5 \ cm^2$) and porous silicon ($1.5 \times 1.5 \ cm^2$) based on n-type Si(100) substrates by using spray pyrolysis method. An aqueous solution of high purity tin chloride ($SnCl_4 \cdot 5H2O$) with concentration of 0.1M was used as starting solution. A small amount (few drops) of concentrated hydrochloric acid (HCl) was added to prevent hydrolysis. For fluorine doping, ammonium fluoride (NH_4F) (99% purity, BHD) dissolved in de-ionized water was added to the starting solution. The doping concentrations was varied of 25 wt. %. The carrier gas flow rate was maintained at pressure of $1 \times 105 \ N. \ m^{-2}$. In both cases the preparation conditions were: the distance between the spray nozzle and the substrates 30 cm. The spray time was 10 s and the spray interval at ~3 min. Totally time to spry a volume of solution was used to produce films and sprayed for 240 sec. The glass substrates temperature was maintained at ($405 \pm 2 \ ^oC$) during the whole spraying process. The thicknesses of the films were determined by weighting method.

$$t = \frac{\Delta m}{\rho \times A} \tag{1}$$

Were Δm is the net weight of film (g), ρ is the density of film (g/cm^3) and A is the area of film (cm^2).
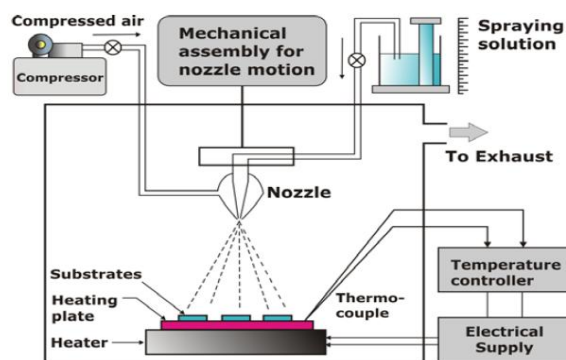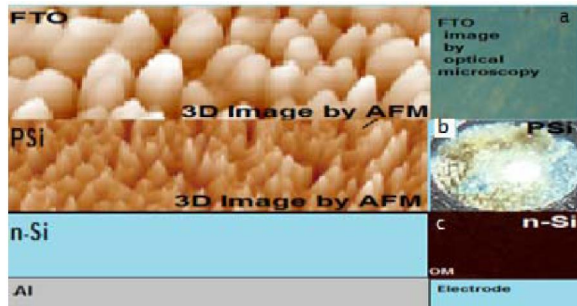

Figure 2 : Schematic diagram of the experimental setup for spray pyrolysis.

Full Paper

This method gives it an approximate thickness for deposited film.

Figure 3 shows the structure of the FTO/PS/n-Si/Al configuration fabricated by planar front Schottky and backside ohmic contacts respectively. The morphological properties of PS layer such as


Figure 3 : Schematic cross section of heterostructures setup of electrical properties measurement, (a) FTO surface image by optical microscopy, (b) PS surface image by camera digital HD Samsung 5x and (c) n-Si surface like mirror image by optical microscopy.

nanocrystalline size, the structure aspect of PS layer and lattice constant have been investigated in this work by using X-ray device (shimadzu - XRD6000) supplied from Shimadzu Company /Japan. The source of X-ray radiation has been Cu-Kα radiation with 0.15406 nm wavelength. The device has been operated at 40 KV and 30 mA emission current. The sample is scanned from (25-80 degrees) 2Theta. In this work, an optical microscopy and AA 3000 Scanning Probe Microscope AFM system have been used. Dark current – voltage FTO/PS/n-Si HJ measurements carried out by applying voltage supplied to the sample from a stabilized D.C. Power supply, type LONG WEI DC-PS-305D 30 range of (-6 to +6) V. The current passing through the device was measured using a UNI-T UT61E Digital Multimeters. The capacitance–voltage C-V measurements are performed at various frequencies by the use of hp4275A-MuTi-frequaency LCR meter –HEWLETT Packard. The C–V characteristic of the diode was also evaluated in the voltage range from -1.2 to 1.2 V at the frequency of 100 kHz. A disc-type ^{60}Co gamma radiation source was used to expose FTO/PS/n-Si HJ. The energy of gamma which is numerically reaching on FTO/PS/n-Si was 7.07mS/hour. Where the activity of the source was 1μc in 2008 and at

using (2014) was 0.6 μc. The distance between the ^{60}Co source and heterojunction was kept at 4 cm during the exposure.

Figure 4(a) the surface morphology of fluorine-doped tin oxide on porous silicon layer substrate.
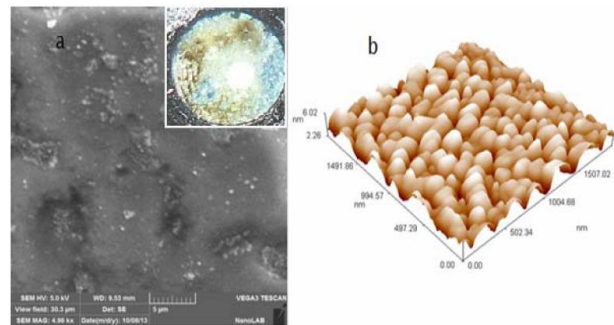
Figure 4 : (a) SEM micrograph of PS layer (right inset the surface image of PS layer by camera digital) prepared by PECE method and (b) 3D AFM images of FTO/PS prepared by chemical spray pyrolysis method

The morphological structure of porous silicon films surface was observed by scanning electron microscopy SEM. it clear the effect of low etching current density from the distribution of cavities etching in surface, inhomogeneous of different etching region. The right inset of Figure 4(a) shows photograph image of porous layer by camera digital HD Samsung 5x. As a result, AFM does only allow imaging of the top end of the pores, which is a general disadvantage of this technique compared with electron microscopy[11]. The advantage of this measurement mode is that the AFM analysis can be done with very small forces[12].

2 and 3 dimension scanned area surface for AFM analysis was 1989nm × 2000nm as shown in Figure4(b) and Figure5. This image shows that the film is homogeneous and has a large number of ellipse aligned grains. The surface was smooth; the root mean square (RMS) of roughness was measured and found to be around 0.734nm and Sa (Roughness Average) of 0.595 nm. The average diameter of FTO was measured from AFM analysis using software and found to be 88.77 nm and it approximately closed to the value which obtained by weighting method 113 nm.

The crystal structure of porous silicon was investigated using X-ray diffraction. The measured XRD patterns are displayed in Figure 6(a). Two diffracted
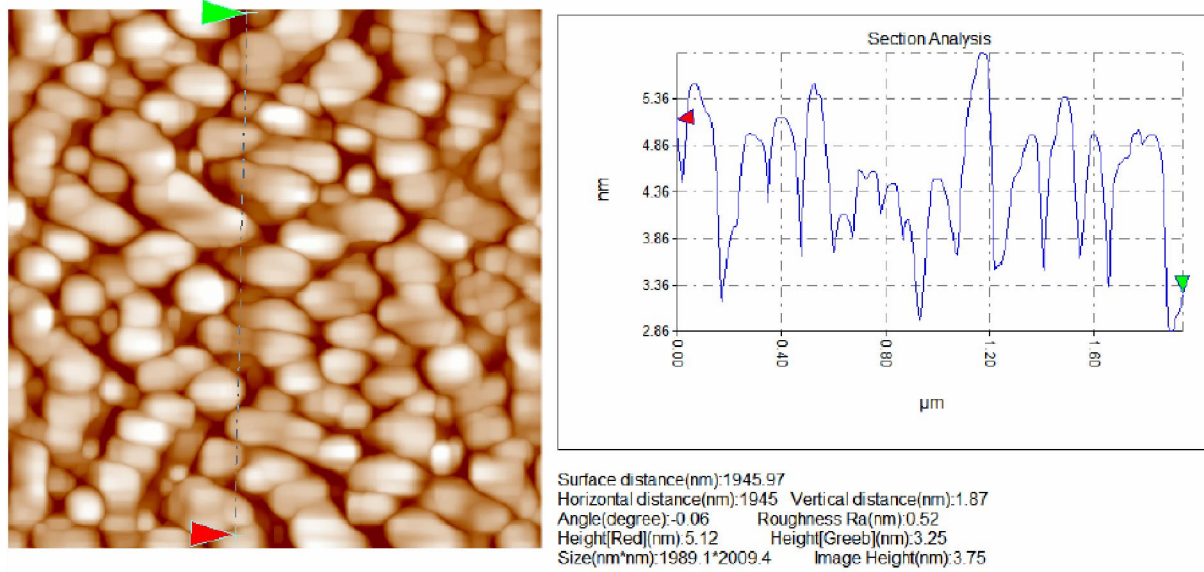
Figure 5 : 2D AFM image of FTO/PS and section analysis

peaks are noticed one has high intensity located at $2\theta = 69.4°$ which is belong to single crystal silicon and the second peak has small intensity located at $2\theta = 69.78°$. XRD was used to investigate the size of the crystallites of the porous silicon. The average grain size (crystallite size) corresponds to the average diameter (L) of the crystallite columns which can be calculated by using Debye–Scherrer formulas shown in equation[11].

$$L = 0.\frac{9\lambda}{FWHM.\cos(\theta)} \qquad (2)$$

Where the FWHM is the full width at the half maximum of the characteristic spectrum in units of radi-

ans, L and λ are in nm. The average diameter of crystallites resulting of the broadening in a spectrum at $\frac{7\,mA}{cm^2}$ etching current density was 68.3nm. A broad reflection indicates that its average crystal size is smaller than that of crystalline silicon according to the Scherrer equation, where the full width half maximum FWHM of c-Si was (0.1239°) while it was (0.1766°) for porous silicon layer.

Right inset Figure 6(b) shows the XRD pattern of non-etched silicon (fresh silicon), it is clear that sharp and high intensity diffracted unique peak noticed at $2\theta = 69.84$ corresponds to (100) plane. A
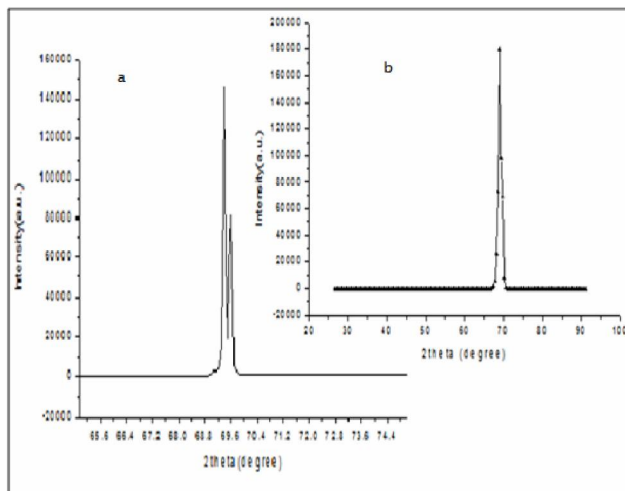

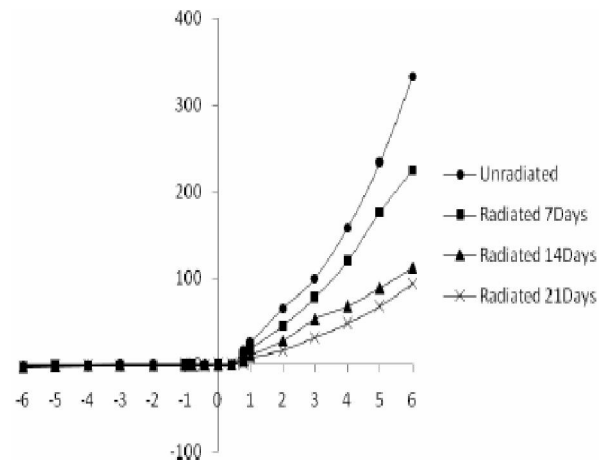**Figure 6 : XRD pattern of porous silicon layer PS and (the right inset) bulk silicon n-Si**

Figure 7 : Unradiation and under radiation for (7, 14 and 21 Days) dark current-voltage characteristics of FTO/PS/n-Si/ Al junction

Full Paper

strong peak of (c-Si) fresh silicon shows a very sharp peak at $2\theta = 69.84°$ oriented only along the (100) direction is observed confirming the monocrystalline structure according to ICDD N 1997and 2011 JCPDS). Figure 7: illustrates the current - voltage of FTO/PS/n-Si/Al when exposed gamma periods of time (7, 14, and 21) respectively. It is clear that the reducing in forward current values were happen when increasing the duration of the radiation. Gamma ray was produced or increased the defects on the surface interfaces of the heterostructures and that agree with[10]. This is attributed to the permanent damage created in the base region reducing the forward current. The effect of gamma radiation on dark (I-V) measurement FTO/PS diode junction formed and investigated by examining the rectification factor, ideality factor, Schottky barrier height, and series resistance. The series resistance will be calculated by the slope at the linear part of the I-V curve. Appling Eq. (3) to determine the ideality factor n; therefore indicate a measure of how close the test sample diode performs relative to ideal diode behavior[13].

$$n = \left(\frac{kT}{q} \frac{d(\ln I)}{dV}\right)^{-1} \quad (3)$$

Usually the large ideality factor of porous layer which is attributed to the roughness of the PS surface and that leads inhomogeneously structure, which acts as a defect in the interface layer between PS/n-Si. It clears the decrease of the forward current with increasing gamma exposures time. That means the structure became have a high series resistance and interface states after radiation, ideality factor n becomes higher and the values of rectification factor will be decreasing as shown in TABLE 1.

The Schottky barrier height may be solved for with the manipulation of the Schottky diode equation to form equation[13]:

$$\emptyset_B = kT/q \ln((AA^T * T^T2)/I_\downarrow s) \quad (4)$$

Our result show that the values of ideality factor n, series resistance R_s, increased after gamma radiation the barrier height values of $\emptyset_{B(F-function)}$ obtained from Nordes are large than that from the standard ln I–V plot and the barrier height values of $\emptyset_{B(H-function)}$ obtained from Cheung's. This is may be due to the strong depend this methods on ideality factor values, where the value of the barrier height of a FTO/PS heterojunction can be determined by Nordes method as follows equation[14]:

$$\emptyset_{B(F-function)} = F(V_{min}) - \frac{nV_{min} - 2V_{min}}{2n} - \frac{(2-n)kT}{n} \frac{q}{q} \quad (5)$$

where $F(V_{min})$ is the minimum value of F(V) and Vmin is the corresponding voltage and The F(V)function is defined as equation[14]:

$$F(V) = \frac{V}{2} - \frac{nkT}{q} \ln\left(\frac{I(V)}{A^*T^2}\right) \quad (6)$$

While the value of the barrier height of a FTO/PS heterojunction can be determined by Cheung's method as follows equation[14]:

$$H(I) = n\emptyset_{B(H-function)} + IR_s \quad (7)$$

And

$$H(I) = V - \frac{nkT}{q} \ln\left(\frac{I}{AA^*T^2}\right) \quad (8)$$

The values of ideality factor n, barrier height $\emptyset_B$ from the standard ln I–V plo t, from Norde's method, from Cheung's method, series resistance , saturation current ,for FTO/PS heterojunction were calculated from the forward I-V characteristics at

TABLE 1 : Electrical parameters of fabricated thickness FTO/PS/n-Si heterojunction as a function duration time after gamma radiation from (I-V) measurement.

| FTO/PS/n-Si/Al	Unradiated	Radiated 7Days	Radiated 14Days	Radiated 21Days
Rectification factor R_f at 3V	1000	154	88	64
Ideality factor (n)	5.7	6.4	6.79	7.16
Barrier higher (I-V) $\emptyset_B$ (Bethe) eV	0.770	0.771	0.772	0.772
Barrier higher (I-V) $\emptyset_{B(H-function)}$ eV	0.768	0.769	0.771	0.772
Barrier higher (I-V)-$\emptyset_{B(F-function)}$ eV	0.79	0.795	0.80	0.82
Series resistance R_s K?	28.2	48.3	88.8	125
Saturation current I_s μA	0.08	0.05	0.02	0.005

Full Paper
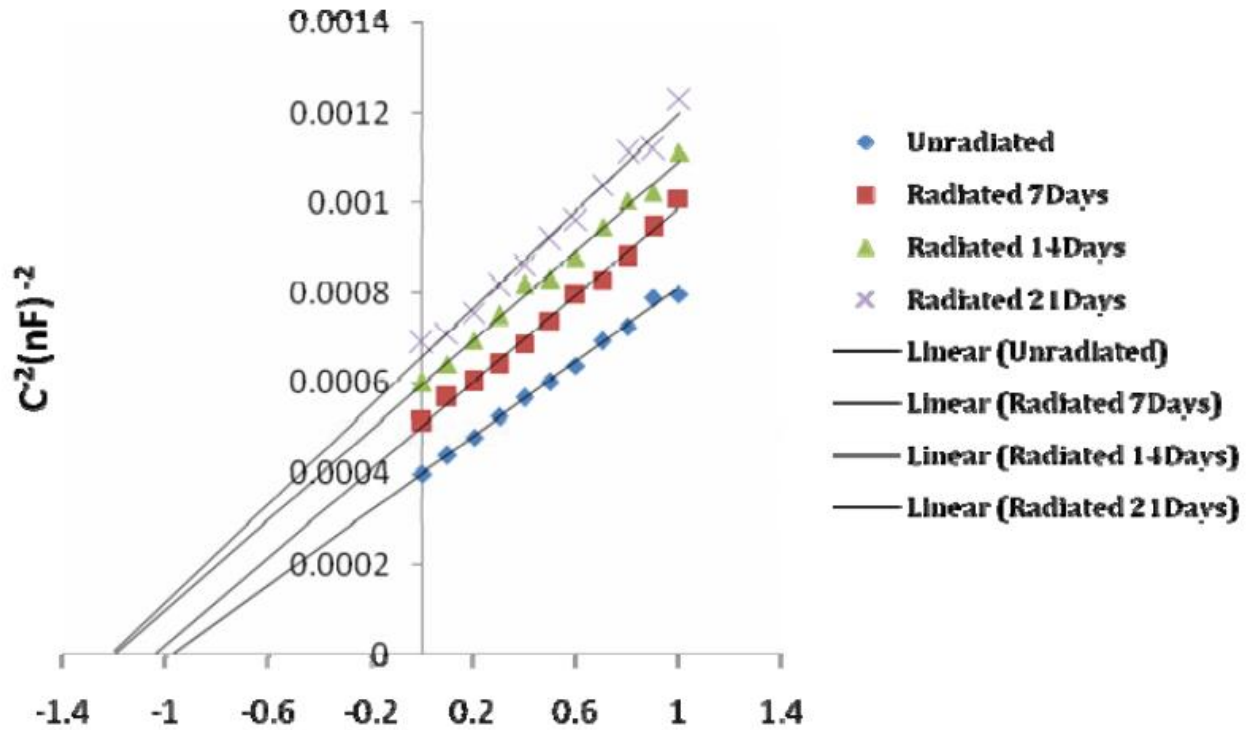
Figure 8 : The effect of duration gamma radiation on the (C^{-2} -V) of the FTO/PS/n-Si heterojunction at frequency of (100 kHz).

TABLE 2 : Electrical parameters of fabricated thickness FTO/PS/n-Si heterojunction as a function duration time after gamma radiation from (C-V) measurement.

FTO/PS/n-Si/Al	Unradiated	Radiated 7Days	Radiated14Days	Radiated 21Days
Built in voltage V_{bi} V	0.98	1	1.19	1.2
Barrier higher (C-V) $\emptyset_B$ eV	1.05	1.07	1.26	1.27
effective density of states concentration cm^{-3}	4E+15	5E+15	5E+15	6E+15

different duration gamma radiation and listed in TABLE 1. As seen I-V Characteristics,the primary electrical parameters such as ideality factor n, rectification factor, saturation current,barrier higher and series resistance were influenced with the presence of gamma radiation.

Figure 8 shows the linear fitting -V plot of the FTOP/PS HJ before and after effect gamma radiation for different time. This plot reveals a good linear relationship before and after gamma radiation for different time and that indicating the abrupt heterojunction theory was domain to the FTO/PS HJ structure. The values of capacitance are decreasing after expose gamma radiation on FTO/PS HJ due to decrease in charge carriers across the junction, so the slope of straight line increase as shown in figure

8. This indicates that the change in interface structural of HJ was happened also, inhomogeneities at the metal–semiconductor interface and that agree with[15]. In TABLE 2 the value of built-in junction potential was calculated from extrapolated plots intersect on bias voltage axis giving the value of built-in junction potential and the effective density of states concentration by slope of the straight line from following equation:

$$\frac{1}{C^2} = \frac{2(V_{bi} + V)}{qN_D\varepsilon_s A^2} \tag{9}$$

where $_s$ the permittivity of Si, the net acceptor concentration in the n-Si, A the junction area, V the applied voltage, and the built-in potential,The obtained values of the barrier height by using Eq. (10) from C-V measurements are higher than those obtained

Full Paper

from I-V measurements[13].

$$\emptyset_B = qV_{bi} + kTLn\left(\frac{N_C}{N_D}\right) \tag{10}$$

CONCLUSION

In this work, we report the results of the morphological and structural of nonporous layer and nanostructure fluoride tin oxides film. Also, we have investigated the influences of duration gamma conditions in the dark I-V and C-V measurement of FTO/PS/n-Si device performance. We note from I-V and C-V characteristics, the primary electrical parameters such as ideality factor n, rectification factor , saturation current ,barrier higher and series resistance were influenced with the presence of gamma radiation. In C-V measurement, it notable changes occurred in Schottky barrier height over the range of duration time gamma radiation.

REFERENCES

[1] H.A.Hadi, R.A.Ismail, N.F.Habubi; N.F.Indian J.Phys, **88**, 59 **(2014)**.

[2] S.Ozdemir, J.Gole; Sens Actuators B., **147**, 247 **(2010)**.

[3] J.Kanungo, H.Saha, S.Basu; Sens Actuators B., **147**, 128 **(2010)**.

[4] H.A.Hadi, I.H.Hashim; Journal of Electron Devices, **20**, 1701 **(2014)**.

[5] A.G.Felipe, R.Urteaga, L.N.Acquaroli, R.R.Koropecki, R.D.Arce; Nanoscale Research Letters **7**, 419 **(2012)**.

[6] A.A.Yadav, E.U.Masumdar, A.V.Moholkar, K.Y.Rajpure, C.H.Bhosale; Physica B., **404**, 1874 **(2009)**.

[7] M.A.Aouaj, R.Diaz, A.Belayachi, F.Rueda, M.Abd-Lefdil; Materials Research Bulletin, **44**, 1458 **(2009)**.

[8] F.A.Garcés, L.N.Acquaroli, R.Urteaga, A.Dussan, R.R.Koropecki, R.D.Thin, Solid Films, **520**, 4254 **(2012)**.

[9] V.Bilgin, I.Akyuzb, E.Ketencic, S.Koseb, F.Atay; Applied Surface Science, **256**, 6586 **(2010)**.

[10] R.M.Yas; Iraqi Journal of Physics, **10**, 71 **(2012)**.

[11] K.Omar, Y.Al-Dour, A.Ramizy, Z.Hassan; Superlattices and Microstructures, **50**, 119 **(2011)**.

[12] D.C.Chang, V.Baranauskas, I.Doi; Journal of Porous Materials, **7**, 349 **(2000)**.

[13] S.M.Sze; Physics of Semiconductor Devices, 2nd Edition, (Willey, New York), **(1981)**.

[14] D.K.Schroder; Semiconductor Material and Device Characterization 3[ed] Edition, (A John Wiley and Sons,Canada), **(2006)**.

[15] A.Cherif, S.Jomni, R.Hannachi, L.Beji; Physica B., **409**, 10 **(2013)**.